NANO LETTERS

2001
Vol. 1, No. 1
8−13

Formation of Platinum Silicide on a Platinum Nanoparticle Array Model Catalyst Deposited on Silica during Chemical Reaction

Ji Zhu[†,‡] and G. A. Somorjai*[,†,‡]

Department of Chemistry, University of California, Berkeley, California 94720, and Material Sciences Division, Lawrence Berkeley National Laboratory, Berkeley, California 94720

Received October 6, 2000

ABSTRACT

Pt nanoparticle model catalysts with 28 ± 2 nm diameters and 100 ± 2 nm square periodicity have been fabricated with electron beam lithography on silica substrates. The reactivity and selectivity of the Pt/SiO_2 array favor dehydrogenation for a cyclohexene and hydrogen mixture to hydrogenation at 100 °C. Experiments with silicon deposited on Pt foil reveal the feasibility of platinum silicide formation at the Pt/SiO_2 interface under reaction condition.

Transition metal catalysts are usually particles in nanometer range deposited on high surface area oxide supports such as silica or alumina. These metal particles often have a broad size distribution in the range of 1 ∼ 100 nm and are randomly located on the support. Previous experiments have identified important atomic level catalyst ingredients that may control reactivity and selectivity are metal catalyst surface structure,[1] metal-oxide interface,[2] and diffusion of surface species between oxide and metal.[3] To conduct controlled experiments that test each of the catalyst ingredients, electron beam lithography (EBL) was used to fabricate model catalysts.[4−5] The EBL fabricated platinum nanoparticle array model catalyst used in this study had metal particles with 28 ± 2 nm diameter and 100 ± 2 nm square periodicity and was supported on a silicon (100) wafer with a layer of 5 ∼ 7 nm thick native oxide. The reactivity of the Pt/SiO_2 array was compared to a Pt foil for cyclohexene hydrogenation and dehydrogenation at 100 °C. The overall reactivity of the Pt particle arrays was higher by a factor of 2, the selectivity toward dehydrogenation was three times higher. In this paper, we also report the formation of platinum silicide under condition encountered during hydrocarbon conversion reaction over Pt/SiO_2 catalyst. Silicon deposited on a clean Pt foil by silane decomposition was oxidized and reduced. Auger electron spectroscopy (AES) was used to monitor the oxidation state of Si and the presence of oxygen. Platinum silicide is a likely modifier of platinum catalysts activity and selectivity during hydrocarbon conversion in the presence of excess hydrogen.

1. Pt Nanoparticle Catalyst Preparation, Characterization, and Reaction Studies. Practical catalysts consist of highly dispersed metal catalyst particles (1∼100 nm) supported on porous active or passive support materials, together forming a complex 3-D structure, which does not lend easy access to surface science characterization methods as a 2-D structure will do. Several methods have since been developed to prepare 2-D model nanoparticle catalysts, for example, laser ablation,[7] spin coating of metal salt solution on oxide support followed by calcinations,[8] evaporation of metal onto oxide support,[9] laser interference nanolithography,[10] electron beam lithography,[4−5] and so forth. The advantages of lithographic fabrication methods include precise control of metal particle size and interparticle distance. In addition, the lithographic approach is not dependent on specific materials, which makes it possible to fabricate catalysts with a wide range of metal and support materials. In all available lithography methods, electron beam lithography has the highest resolution with a minimum diameter down to 10 nm and interparticle distance down to 50 nm, which makes electron beam lithography the ideal choice for fabricating model catalyst that mimics the real catalyst. By changing the size of metal particles in the relevant regime, size effects on catalytic activity can be studied. The metal−support interaction can also be studied

* To whom correspondence should be addressed. E-mail: Somorjai@cchem.berkeley.edu.
[†] Department of Chemistry, University of California.
[‡] Material Sciences Division, Lawrence Berkeley National Laboratory.

10.1021/nl005512q CCC: $20.00
Published on Web 11/28/2000

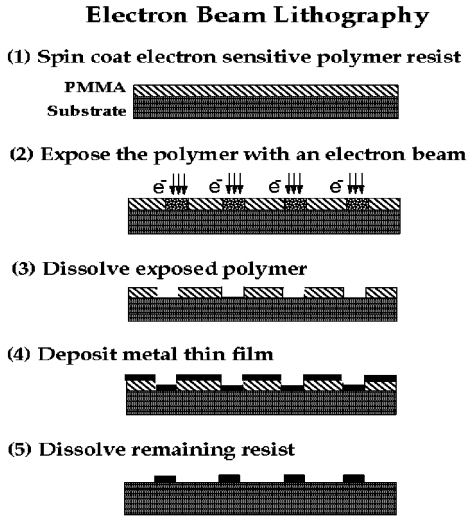

Figure 1. Schematic procedure of electron beam lithography.

in a more controlled way by systematically varying the support materials.

The electron beam lithography is conducted on a Leica nanowriter machine. A scheme of the process is shown in Figure 1. Briefly, a thin layer of 350K PMMA was spin-coated onto a Si (100) wafer with 5−7 nanometer native SiO_2 on the surface. A square pattern was then "written" into the polymer layer with a highly collimated electron beam generated by a field emission source. With a beam current of 600 pA and accelerating voltage of 100 kV, the beam diameter was approximately 3 nm. A dose of 2500 μC/cm^2 was used to expose the PMMA, resulting in a dwell time of about 6 μs at each particle site. After dissolving the exposed polymer, a 15 nm Pt film was then deposited on the surface through the polymer mask by electron beam evaporation. Finally, the remaining resist was removed by dissolution in acetone and the metal particles of the prescribed pattern remained on the substrate. With this high degree of spatial resolution, 36 mm^2 array with approximately 10^9 particles were produced in the time period of several hours. Atomic force microscopy (AFM) and scanning electron microscopy (SEM) were used to characterize the sample. AFM images were taken with a Park Scientific Instruments autoprobe in contact mode in ambient atmosphere. SEM images were taken with a Joel 6340F field emission scanning electron microscope. The images obtained by AFM and SEM are shown in Figure 2. The SEM image showed the particle size to be around 28 ± 2 nm with 100 ± 5 nm spacing. AFM topography image showed the particles to be 15 nm high, and the spacing was 100 nm. Due to the convolution of the tip shape and particle shape, no attempt was made to extract particle size information from the topography image.

Sample cleaning, preparation, characterization by Auger electron spectroscopy (AES) and temperature programmed desorption (TPD), reactivity study were performed in an ultrahigh vacuum (UHV) chamber with an internal high-pressure reaction cell. The chamber was equipped with a quadrupole mass spectrometer, a double-pass cylinder mirror analyzer, an ion gun, a 330L/s turbomolecular pump and a 400 L/s ion pump. Typical base pressure of well-baked

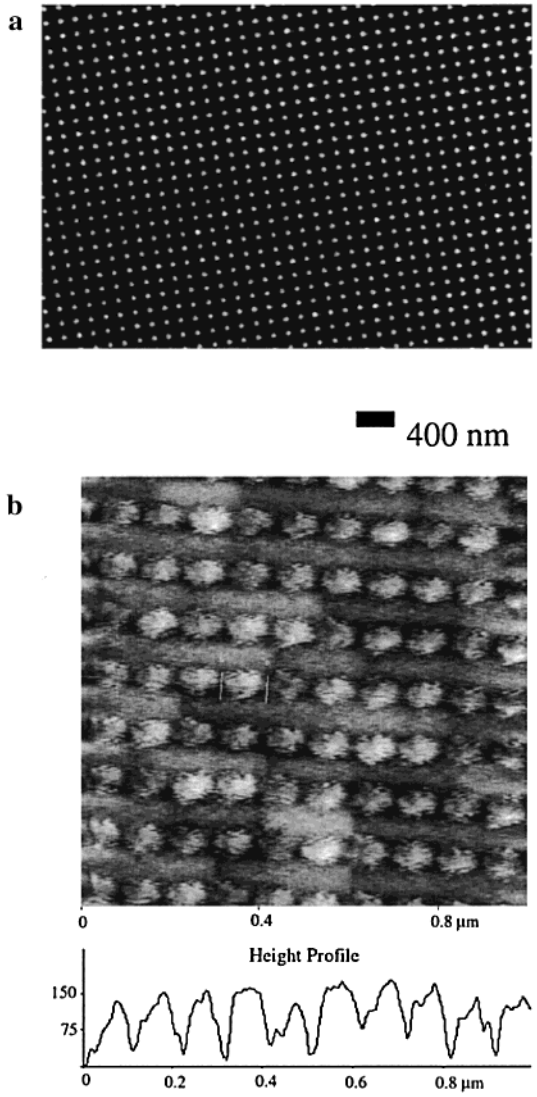

Figure 2. (a) Field emission scanning electron microscope image of the catalyst. The particle diameters were 28 ± 2 nm and interparticle distance was 100 ± 5 nm. (b) 3-D presentation of the AFM image of the catalyst. The particles were 15 nm high and had a periodicity of 100 nm.

chamber was 5×10^{-10} Torr. Between cleaning cycles and reactions, the typical pressure was 2×10^{-9} Torr. The model catalyst was mounted onto a ceramic heater by Ta clips. With the heater and liquid nitrogen cooling loop, the sample can be heated to 1000 °C and also cooled to −90 °C. The clean sample was prepared by repeat cycle of 1 kV Ne^+ sputtering, oxygen treatment (1×10^{-6} Torr) at 500 °C and subsequent anneal at 650 °C to remove any PtO_x that may have formed during the O_2 treatment. Analysis by Auger electron spectroscopy showed that this procedure was capable of preparing an atomically clean Pt sample. A reaction study was conducted at 100 °C under atmospheric pressure with the reaction cell closed by a hydraulic system at 2300 psi, while keeping the rest of the chamber still under UHV. The volume of the batch reactor was 200 mL, which was recirculated by a pump at flow rate of 15 mL/min. The reaction gas composition was 1.5 Torr cyclohexene, 15 Torr H_2, and 755 Torr Ne makeup gas, premixed in a gas manifold. The

cyclohexene (purity = 99.7%) was purchased from Aldrich and further purified by three freeze−pump−thaw cycles before reaction to remove any minor impurities. During the reaction, the reactant and product mixture was sampled every 13 min using an automatic sampling valve, which was on the reaction loop and attached to a gas chromatograph. The hydrocarbons were separated in a 50 m alumina capillary column and monitored by a flame ionization detector.

Cyclohexene dehydrogenation and hydrogenation reaction can take place readily at 100 °C, with benzene and cyclohexane as major products. To characterize the reaction, the turnover number (molecule/site), selectivity, and deactivation rates were considered. The reactivity of the Pt nanoparticle catalyst, with 28 nm diameter particles, 15 nm height, and 100 nm spacing was compared to the reactivity of a 0.06 cm^2 Pt foil (purity > 99.99%). A bare SiO_2/Si (100) wafer was used for background activity correction. The surface area of Pt on the array and foil was measured with CO TPD. The primary difference between the Pt particle array and Pt foil was the presence of Pt−SiO_2 interface. For particles of this size, with around 100 000 atoms in each particle, the electronic structure of the metal was not considered different from that of bulk Pt. Due to the curvature of the particles, their surface may have a higher density of step and kink sites than the foil.

The turnover numbers were larger on the Pt array than those on the foil for both hydrogenation and dehydrogenation (Figure 3). As seen by the turnover number, the selectivity of the nanoparticle array was over three times higher toward the dehydrogenation of cyclohexene than the foil. This trend was true for all of the reactions on the nanoparticle array. Defining deactivation as the ratio of the slope of cyclohexene consumption curve from the first 13 min to the slope between 130 and 180 min of reaction time, the particles showed the same rate of deactivation as the Pt foil. Nanoparticle catalysts can have quite different kinetics from single crystals due to kinetic effects alone (i.e., interfacet diffusion, spillover, adsorbate induced reshaping, etc.). These effects are especially important in the case of rapid reactions occurring far from adsorption desorption equilibrium.[11] In our cases, the reaction took place in recirculating high-pressure reaction gases, and the total turn over was about a few percent, the adsorption−desorption equilibrium should always be maintained on the catalyst. However, hydrogen spillover from platinum particle to the oxide surface could be one possible candidate for the selectivity difference, as well as increased step and kink site density on the nanoparticles and metal-oxide interface. The interface is the most interesting because Pt−Si−O overlayers have been show to influence catalytic activity.[12] Besides, XPS studies on the effect of Ne sputtering on platinum thin film deposited on SiO_2/Si revealed platinum silicide formation when the boundary of Pt layer, and the underlying silicon or silica was broken, as shown in Figure 4. Platinum silicide formation by ion mixing has been reported and studied extensively.[13] It is quite possible that platinum silicide will form on the Pt−SiO_2 interface during the cleaning process, in which the platinum nanoparticles underwent repeated ion sputtering. The interface silicide could be a component of a new active site, which is responsible for the kinetic difference observed on the nanoparticle catalysts.

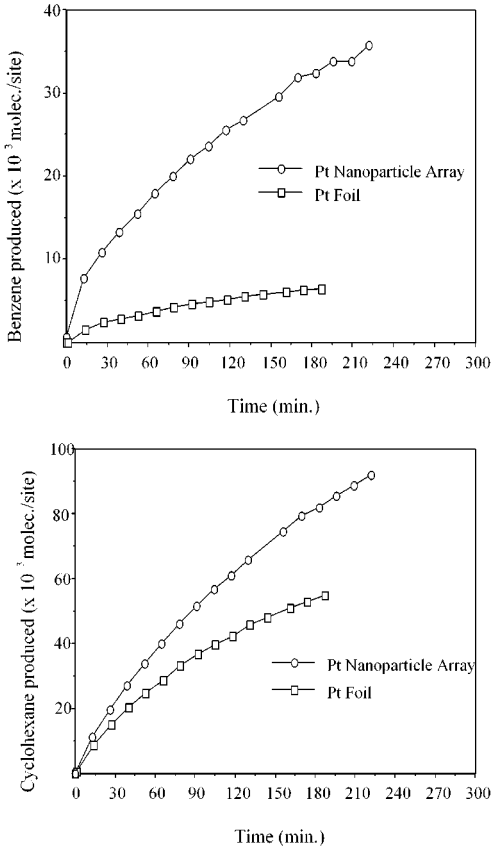

Figure 3. Turnover numbers (molec/site) for benzene and cyclohexane produced from cyclohexene on the nanoparticle array and a Pt foil (0.06 cm^2).

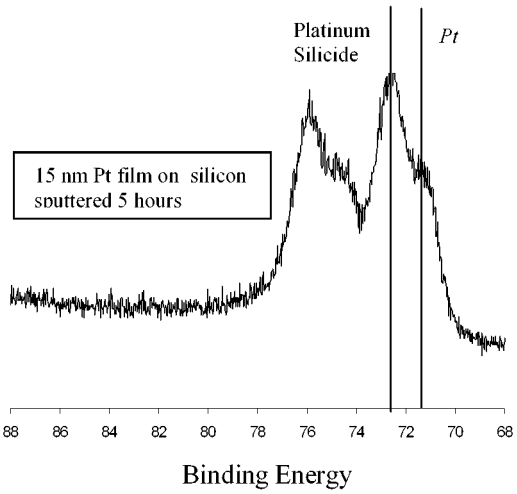

Figure 4. XPS spectrum of a sputtered Pt film evaporated onto Si (100) wafer with 5 ∼ 7 nm native oxide. The film underwent 5 h of 1 kV, 1 μA Ne^+ sputtering.

2. Silicon Deposition on Pt Foil. To study the formation of silicide on Pt, silane was used to deposit silicon on to a Pt foil. Silane (purity = 99.85%) was purchased from Aldrich and used without further purification. Silane dissociates readily on Pt surface even at −160 °C,[14] producing SiH_x and

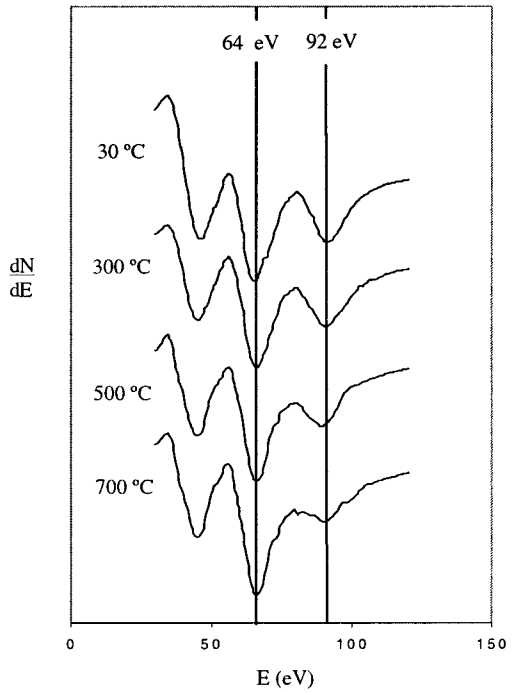

Figure 5. Evolution of Auger spectra of a platinum sample flash annealed to the indicated temperatures successively. The sample started with 6 L exposure to silane at room temperature, which produced a saturation coverage. Then the sample was flash annealed and cooled, and the Auger spectrum was taken.

adsorbed hydrogen atoms, which recombine and desorb from the surface at about −23 °C. Numerous studies have shown that silicon and platinum react readily at room temperature and form silicides of different stoichiometry depending on the condition and the abundance of the reacting elements.[15,16] Of the 16 different Pt silicide phases characterized by X-ray-based methods,[18] there are 5 stable bulk platinum silicide phases that can exist from room temperature to 800 °C.[19] Previous results show that the stable phase for a thin platinum film deposited on silicon wafer is the silicon rich PtSi phase,[15−16] whereas for the impurity, Si segregated on Pt under UHV annealing, the stable phase is a platinum rich Pt_2Si phase.[17] A recent STM study of silane dosed platinum (111) and (100) single crystals showed the existence of 7 and 4 surface platinum silicide phases on Pt (111) and Pt (100) respectively[20−21]. Auger spectra of the Pt foil under different silane exposure at room temperature showed that the silicon uptake saturated at about 6 L silane exposure. After saturation coverage of silane was reached, the sample was flashed to different temperatures and cooled to room temperature, at which time Auger spectra were taken (Figure 5). The most significant feature of these spectra was the decreasing AES intensity of the Si 92 eV peak and increasing AES intensity of the Pt 64 eV peak. It was known from previous study that no silicon-containing species desorb from the Pt surface during the temperature ramping.[14] The Pt−Si phase diagram[19] shows that Si has moderate solubility in Pt of about 2% at 600 °C and about 3% at 800 °C. The attenuation of the Si signal from the surface can be attributed to Si diffusion into Pt bulk. Due to the diffusion process, the thermal history of the sample strongly determines the surface concentration of Si and, therefore, the physical and chemical properties of the surface.

3. Chemical Stability of Silicide on Pt Foil. The chemical stability of the silicide on Pt surface in oxygen was studied by exposing the samples to 1×10^{-6} Torr O_2 or 15 Torr O_2 at different temperatures. Although the Si AES peak at 92 eV does not shift when elemental silicon forms silicide, it does show a significant shift to lower energy upon oxidation with SiO shifting to 85 eV and SiO_2 shifting to 76 eV;[22] therefore, AES is used to characterize the oxidation state of the Si on the surface (Figure 6a). Before oxidation, saturation coverage of Si was deposited on a Pt foil at room temperature, then the sample was flash annealed at 700 °C. During the initial 10 min of heating in 1×10^{-6} Torr O_2 at 700 °C, the silicon atoms continued to diffuse into the Pt bulk. After 20 min, a shoulder appeared around 84 eV, indicating that the silicon on the surface was oxidized. Longer heating helped bring more Si out of the bulk and shift the silicon peak to a lower value as the 82 eV peak continued growing even after 85 min of heating. At higher temperature or oxygen pressure, the oxidation is facilitated. Heating the sample at 800 °C in 1×10^{-6} Torr O_2, 10 min is enough to oxidize the surface silicide. Figure 6b showed the result of oxidation in 15 Torr O_2. The sample was exposed to 6 L silane at room temperature and then annealed at 300 °C. The surface silicide is readily oxidized at 300 °C. Further experiments showed that the surface silicide can be oxidized at 100 °C in 100 Torr O_2. Both 1×10^{-5} Torr and 10 Torr H_2 were then tried to reduce the oxidized silicon on the surface, and showed the same behavior, so only the low-pressure reduction results are presented in Figure 7. After 10 min heating in 1×10^{-5} Torr H_2 at 700 °C, the silicon peak showed a shoulder at around 91 eV, signaling the presence of reduced silicon on the surface. Further heating in H_2 at successively higher temperature up to 850 °C reduced essentially all of the oxidized silicon, as the O peak at 510 eV disappeared. Other studies reported silicon oxides decomposed at temperatures above 1000 °C,[22] hence the presence of hydrogen significantly reduced the temperature required to decompose the silicon oxide. In a typical catalytic reforming plant, the operation conditions are 430−520 °C and 145−870 psi and hydrogen-to-hydrocarbon ratio varies from 5 to 10.[23] In addition, nanometer metal clusters can reduce SiO_2 under the same condition, where no reaction happens between the bulk metal and SiO_2.[24] There are reasons to believe that, under those conditions, Pt nanoparticle could reduce the silicon oxide support nearby to silicon and platinum silicide might be formed on the metal particle oxide interface. After the reduction, the silicon on Pt surface showed quite different oxidation behavior as compared to freshly dosed silicide. Silicon peak showed a very small shift of 2 eV toward lower energy after 10 min oxidation in 1×10^{-6} Torr O_2 at 800 °C, and the oxygen uptake was much less. There are several possible explanations. First, after reduction, a new platinum silicide phase may form on the surface, which has a higher resistance to oxidation. Second, the silicon deposited from silane forms 3-D islands on the Pt surface; therefore, some bare Pt atoms are left on the

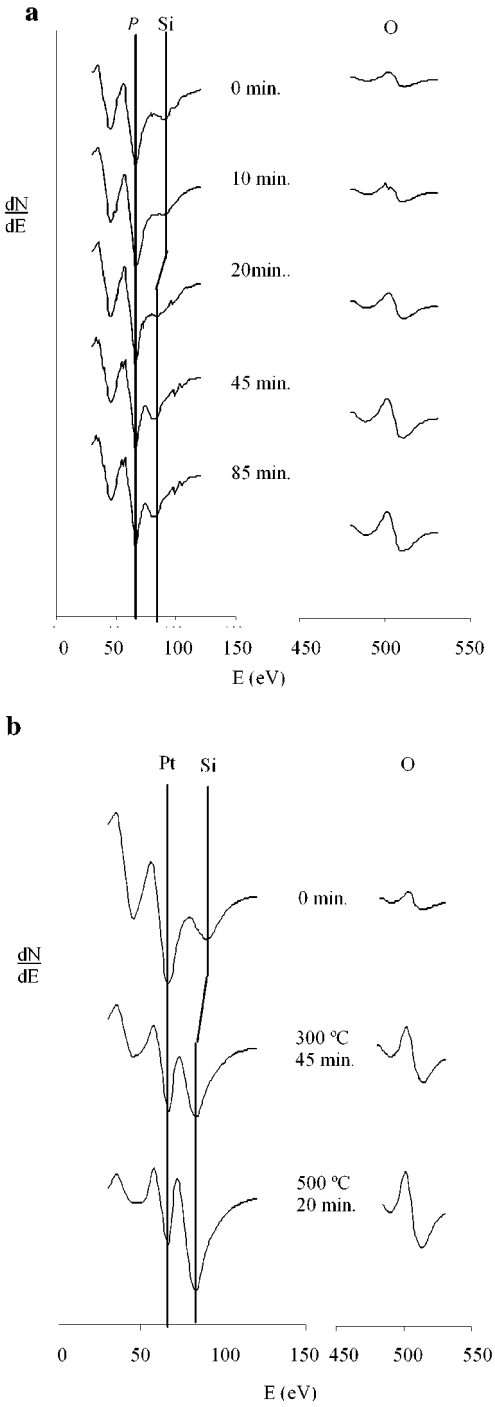

Figure 6. (a) Low-pressure O_2 treatment. The sample was given a saturation coverage dose at room temperature, flash annealed to 700 °C, then heated in 1×10^{-6} Torr O_2 at 700 °C for the indicated time on the graph. There was some oxygen on the surface even before O_2 treatment due to water vapor in the UHV chamber. In later experiment, the presence of this oxygen could be avoided by dosing silane at 500 °C. (b) High-pressure O_2 treatment. After a saturation exposure to silane at room temperature followed by flash annealing at 300 °C, the sample was heated in 15 Torr O_2 under indicated condition on the graph.

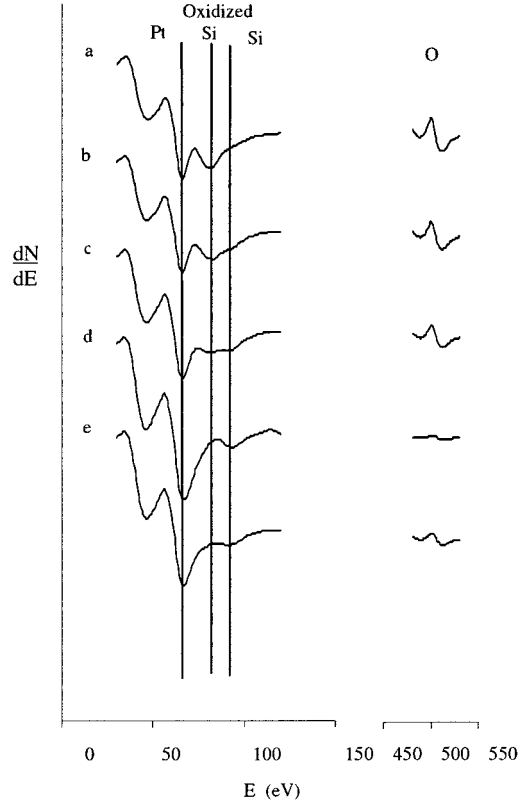

Figure 7. AES series of low-pressure H_2 reduction of $Pt-SiO_x$. After saturation exposure to silane at room temperature, the platinum foil was treated in 1×10^{-6} Torr O_2 at 800 °C for 10 min (a), then successively treated in 1×10^{-5} Torr H_2 at (b) 700 °C for 10 min., (c) 800 °C for 10 min., and (d) 850 °C for 30 min. Finally, the sample was treated in 1×10^{-6} Torr O_2 at (e) 800 °C for 10 min. The absence of oxide formation indicates the resistance of the silicide to oxidation in this circumstance.

surface, which can catalyze the oxidation of the Si by dissociating molecular O_2. However, after reduction at higher temperature, silicon atoms diffuse across the surface, form silicide with Pt and inhibit the ability of Pt to dissociate O_2. Third, the silicon atoms constantly diffuse into the Pt bulk due to its solubility, therefore, the surface silicon concentration is much smaller, and the oxygen uptake is correspondingly less. Also, clean platinum has an AES peak at 93 eV, although small. To test the possibilities, a 6 L dosage of silane was deposited on the Pt surface at 500 °C and subsequently annealed at 850 °C for 10 min. This sample is easily oxidized by 1×10^{-6} Torr O_2 at 800 °C, so the second reason can be ruled out. Further experiments are needed to elucidate the mechanism. CO adsorption is also affected by the presence of silicon on Pt surface, the results of which will be shown in another paper.

In summary, Pt nanoparticle is fabricated with electron beam lithography and used as model catalyst for the reaction of cyclohexene hydrogenation and dehydrogenation at 100 °C. Compared to the reactivity on a Pt foil, the Pt/SiO_2 model catalysts showed higher overall turnover and higher selectivity toward dehydrogenation, indicating that the dehydrogenation pathway may have been facilitated by the $Pt-SiO_2$ interface. XPS revealed the presence of platinum silicide on sputtered Pt film supported on silicon. Silane then was used to synthesize silicide on a clean Pt foil, AES studies showed silicide formation was quite feasible under reaction condition. Further experiment will investigate the catalytic behavior of the silicide in hydrocarbon conversion.

Acknowledgment. This work was performed under the auspices of the Office of Basic Energy Sciences, Materials Sciences Division of the US Department of Energy under Contract No. DE-AC03-76SF00099.

References

(1) Somorjai, G. A. *Introduction to Surface Chemistry and Catalysis*; Wiley: New York, 1994.
(2) Vurens, G. H.; Salmeron, M.; Somorjai, G. A. *Prog. Surf. Sci.* **1989**, *32*, 333.
(3) Conner, E. C.; Falconer, J. L. *Chem. Rev.* **1995**, *95*, 975.
(4) Wong, K.; Johansson, S.; Kasemo, B. *Faraday Discuss.* **1996**, *105*, 237.
(5) Jacobs, P. W.; Ribero, F. H.; Somorjai, G. A.; Wind, S. J. *Catal. Lett.* **1996**, *37*, 131.
(6) Eppler, A. S.; Zhu, J.; Anderson, E. A.; Somorjai, G. A. *Top. Catal.* **2000**, *13*, 33.
(7) Paszti, Z.; Horvath, Z. E.; Peto, G.; Karacs, A.; Guczi, L. *Appl. Surf. Sci*. **1997**, *109/110*, 67.
(8) Doornkamp, C.; Laszlo, C.; Wieldraaijer, W.; Kuipers, E. W. *J. Mater. Res.* **1995**, *10*, 411.
(9) Henry, C. R. *Surf. Sci. Rep.* **1998**, *31*, 231.
(10) Schildenberger, M.; Bonetti, Y.; Aeschlimann, M.; Scandella, L.; Gobrecht, J.; Prins, R. *Catal. Lett.* **1998**, *56*, 10.
(11) Zhdanov, V. P.; Kasemo, B. *Surf. Sci. Rep.* **2000**, *39*, 25.
(12) Keck, K.-E.; Kasemo, B. *Surf. Sci.* **1986**, *167*, 313.
(13) (a) Tsaur, B. Y.; Liau, Z. L.; Mayer, J. W. *Appl. Phys. Lett.* **1979**, *34*, 168. (b) Tsaur, B. Y.; Mayer, J. W.; Tu, K. N. *J. Appl. Phys.* **1980**, *51*, 5326. (c) Tsaur, B. Y.; Liau, Z. L.; Mayer, J. W. *Phys. Lett.* **1979**, *71A*, 270.
(14) Nashner, M. S.; Bondos, J. C.; Hostetler, M. J.; Gewirth, A. A.; Nuzzo, R. G. *J. Phys. Chem. B* **1998**, *102*, 6202.
(15) (a) Das, S. R.; Sheergar, K.; Xu, D. X.; Naem, A. *Thin Solid Films*, **1994**, *253*, 467. (b) Donaton, R. A.; Jin, S.; Bender, H.; Zagrebnov, M. *Micro. Eng.* **1997**, *37/38*, 507.
(16) (a) Ruterana, P.; Solt, K.; Buffat, P.-A. *Surf. Sci.* **1991**, *251/252*, 150. (b) Poate, J. M.; Tisone, T. C. *Appl. Phys. Lett.* **1974**, *24*, 391.
(17) (a) Cardillo, M. J.; Becker, G. E. *Surf. Sci.* **1980**, *99*, 269. (b) Tsong, T. T.; Wang, S. C.; Liu, F. H.; Cheng, H.; Ahmad, M. *J. Vac. Sci. Technol. B* **1983**, *1*, 915.
(18) *Pearson's Handbook of Crystallographic Data for Intermetallic Phases*, 2nd ed.; ASM International: Materials Park, OH, 1991; Vol. 4.
(19) *Moffatt's Handbook of Binary Phase Diagrams*; Jack, H. Ed.; Genium Pub. Corp.: Westbrook, Schenectady, NY, 1997.
(20) Bondos, J. C.; Gewirth, A. A.; Nuzzo, R. G. *J. Phys. Chem. B* **1999**, *103*, 3099.
(21) Bondos, J. C.; Drummer, N. E.; Gewirth, A. A.; Nuzzo, R. G. *J. Am. Chem. Soc.* **1999**, *121*, 2498.
(22) Ko, C. S.; Gorte, R. J. *Surf. Sci.* **1985**, *155* , 296.
(23) *Encyclopedia of Chemical Technology*, 3rd ed.;, John Wiley & Sons: New York, 1980; Vol. 17.
(24) van den Oetelaar, L. C. A.; van den Oetelaar, R. J. A.; Partridge, A.; Flipse, F. J.; Brongersma, H. H. *Appl. Phys. Lett.* **1999**, *74*, 2954.

NL005512Q